https://doi.org/10.62753/ctp.2002.21.3.3

Fabrizio Fiori[1], Emmanuelle Girardin[2], Alessandra Giuliani[3], Franco Rustichelli[4]
INFM - Istituto Nazionale per la Fisica della Materia, U.d.R. Ancona, Italy
Istituto di Scienze Fisiche, University of Ancona, Via Ranieri 65, 60131 Ancona, Italy

RESIDUAL STRESSES IN METAL MATRIX COMPOSITES: EXPERIMENTAL DETERMINATION BY NEUTRON DIFFRACTION

Neutron diffraction experiments are presented, for the evaluation of residual stresses in metal matrix composites (MMC) samples and components, induced by different thermo-mechanical treatments and operating conditions. After a brief description of fundamental theory of residual stresses in MMCs, and some remarks on the experimental technique, results are presented concerning experiments on tensile and fatigued specimens as well as on real components.

From experimental data, the different contributions to the measured stress, namely macrostresses and elastic and thermal mismatch microstresses, were evaluated. Finally, experimental results are compared to finite element calculations.

NAPRĘŻENIA RESIDUALNE W KOMPOZYTACH METALOWYCH WYZNACZONE DOŚWIADCZALNIE METODĄ DYFRAKCJI NEUTRONOWEJ

Przedstawiono badania dyfrakcji neutronowej wykonane w celu określenia rozwoju naprężeń residualnych w kompozytach metalowych. Badania przeprowadzono zarówno dla próbek kompozytowych, jak i komponentów, przy uwzględnieniu różnych warunków eksploatacyjnych, jak i zabiegów cieplno-mechanicznych. Podano zwięzły opis fundamentalnej teorii naprężeń residualnych w kompozytach metalowych oraz skomentowano niektóre techniki eksperymentalne (rys. 1). Badania przeprowadzono dla tarcz hamulcowych wykonanych z kompozytów na osnowie aluminiowej (AA359) umacnianej 20% SiC. Analizowano materiał w stanie pierwotnym oraz naprężenia residualne określone po testach rozciągania i pełzania. Ostatecznie badania na finalnym elemencie w postaci tarczy hamulcowej przeprowadzono zarówno przed, jak i po testach hamowania (rys. rys. 2 i 3). Z danych doświadczalnych oszacowano różne rozkłady obliczonego naprężenia, a mianowicie makronaprężenia oraz sprężyste i niedopasowanie mikronaprężeń cieplnych. Wszystkie wyniki uzyskane z analiz porównano z obliczaniami wykonanymi metodą elementów skończonych.

Określono, że po procesie zmęczenia naprężenia cząstkowe w krytycznych punktach bębna hamulcowego dążyły do zaniku. W odlewanych próbkach kompozytowych AA359+20%SiC nie obserwowano żadnych makronaprężeń, natomiast makronaprężenia obecne w bębnie hamulcowym pochodziły prawdopodobnie z samego procesu wytwarzania. W dolnej części bębna makronaprężenia były prawie takie same zarówno przed, jak i po testach, natomiast wzrosły na ściance i zmalały w uszkodzonych częściach po zakończonych testach hamowania. Niedopasowanie mikronaprężeń cieplnych w bębnie hamulcowym było natomiast takie samo jak w materiale w stanie pierwotnym.

THEORY OF NEUTRON DIFFRACTION MEASUREMENTS OF RESIDUAL STRESSES IN COMPOSITES

The results of a residual stress measurement by neutron diffraction should be considered an average over all the crystallites in the gauge volume which satisfy the Bragg condition

$$\lambda = 2\, d_{hkl} \sin\theta \qquad (1)$$

for the investigated (*hkl*) lattice planes. In eq. (1) d_{hkl} is the interplanar distance and 2θ the diffraction angle with respect to the incoming beam direction (Fig. 1).

The measured strain is defined as

$$\varepsilon_{hkl} = \frac{d_{hkl} - d_{0,hkl}}{d_{0,hkl}} \qquad (2)$$

where $d_{0,hkl}$ is the unstrained interplanar distance. The measured strain direction is parallel to the exchanged wave vector $\mathbf{Q} = \mathbf{k} - \mathbf{k_0}$, where $\mathbf{k_0}$ is the wave vector of incoming neutrons and $\mathbf{k}$ is the same quantity for diffracted neutrons, and, as shown in Figure 1, it is perpendicular to the investigated (*hkl*) planes.

In general, in order to obtain the complete strain (and stress) tensor, measurements in at least 6 different spatial directions should be performed, or more if experimental errors can not be neglected [1]. Anyway, the procedure is rather simple if the sample geometry allows a reasonable *a priori* definition of the strain principal directions. In fact, in this case measurements in these three directions (e.g. *X*, *Y* and *Z*) are sufficient to

[1] dr, [2] dr, [3] dr, [4] prof.

determine the global strain state, and stresses can be calculated by means of the Hooke's law

$$\sigma_X = \frac{E}{(1-2\nu)(1+\nu)}\left[(1-\nu)\varepsilon_X + \nu(\varepsilon_Y + \varepsilon_Z)\right] \qquad (3)$$

where E and ν are the Young modulus and the Poisson ratio of the material, respectively (corresponding relations for the Y and Z stress components are obtained by simple permutations of X, Y and Z indices).

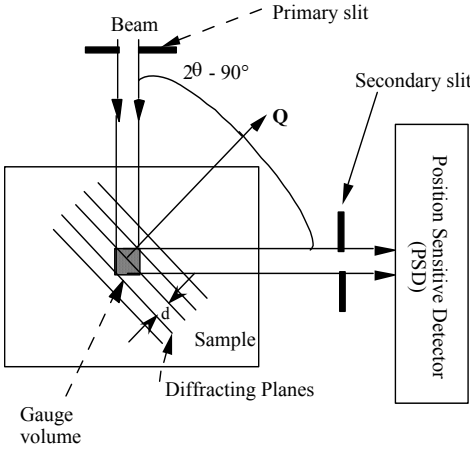

Fig. 1. Lay-out of a neutron diffraction experiment for residual stress measurements

Rys. 1. Schemat doświadczenia dyfrakcji neutronowej do obliczeń naprężeń cząstkowych

For a composite material, the **total measured stress** ($\boldsymbol{\sigma}_{tot}$, averaged over the gauge volume) in each phase can be splitted into three contributions:

- A **macrostress** ($\boldsymbol{\sigma}_{macro}$), which varies smoothly on a spatial scale corresponding to many grains. This component is the same for both phases and is of prime interest for what concerns the material mechanical properties for engineering applications. Stresses of this type may be mechanically applied or thermally induced and are detectable by destructive techniques such as hole-drilling.
- An **elastic mismatch microstrain** ($\boldsymbol{\sigma}_{mE}$), varying on a scale characteristic of the inhomogeneous structure. It is due to difference in elastic constants of the two phases, and represents the load transfer to the stiffer phase (e.q. SiC reinforcement). It is directly proportional to the macroscopic stress field.
- A **thermal mismatch microstrain** ($\boldsymbol{\sigma}_{mT}$), which is due to difference in thermal expansion coefficients of the two phases. Plastic deformation in the matrix or cooling the material from high temperatures (for instance during its production) will cause an average tensile stress in the Al matrix and a compressive one in the SiC reinforcement. This kind of stress is expected to be isotropic (hydrostatic).

Thus the following relation holds for both phases (i):

$$\boldsymbol{\sigma}^i_{tot} = \boldsymbol{\sigma}_{macro} + \boldsymbol{\sigma}^i_{mE} + \boldsymbol{\sigma}^i_{mT} \qquad (4)$$

The macrostresses can be calculated from the measured stresses in both phases as follows:

$$\boldsymbol{\sigma}_{macro} = f\boldsymbol{\sigma}^{SiC}_{tot} + (1-f)\boldsymbol{\sigma}^{Al}_{tot} \qquad (5)$$

where f is the volume fraction of the SiC reinforcement.

The elastic mismatch microstress is related to the macrostress by means of the following equation:

$$\boldsymbol{\sigma}^i_{mE} = \mathbf{B}^i\, \boldsymbol{\sigma}_{macro} \qquad (6)$$

where $\mathbf{B}^i$ is a tensor depending on the reinforcement particle shape and on the elastic constants of the two phases. It has been calculated and tabulated in [2] for the AA2124+SiC system, on the basis of the Eshelby's „equivalent homogeneous inclusion" model [3].

Finally, the thermal mismatch microstress in each phase can be calculated by means of eq. (4).

EXPERIMENTAL RESULTS

An Al matrix brake drum reinforced with 20% of SiC has been studied. The cast material has been analysed, tensile and fatigue tests have been performed and residual stresses determined in the test samples. The final component before and after bench test has been studied and all the results obtained analysed and compared with calculation.

AA359+20%SiC cast sample (PM3)

The sample is free of macrostresses, the elastic mismatch microstresses are negligible. The main contribution to the measured stress is the thermal mismatch microstress which is ≈100 MPa in the Al matrix and ≈ –400 in the SiC reinforcement.

AA359+20%SiC T6 – 0.2% strain (PM4)

The sample is free of macrostresses, the elastic mismatch microstresses are negligible. The main contribution to the measured stress is the thermal mismatch microstress which are lower than in the cast block: ≈20 MPa in the Al matrix and ≈ –150 in the SiC reinforcement.

AA359+20%SiC fatigue specimens

All the specimens are free of macrostresses, and the elastic mismatch microstresses are negligible. The errors are around 100 MPa.

	Thermal Mismatch Micro-stress, MPa			
	Al		SiC	
	Radial	Axial	Radial	Axial
359 MMC, stress = 65 MPa $2.91 \cdot 10^6$ cycles failed (10÷21)	274	188	–1090	–750

359 MMC, stress = 70 MPa $6.97 \cdot 10^4$ cycles failed (10÷19)	240	245	–962	–981

The stresses are higher in the fatigue specimens than in the cast block. The stresses don't seem to be modified by the number of cycles.

RESIDUAL STRESS MEASUREMENT IN A AA359+20%SiC BRAKE DRUM

Measurement before bench test

The 1st point is at the surface of the „wall". The residual stresses has been measured by X-ray diffraction, so the hoop stress is 0 (Figures 2 and 3).

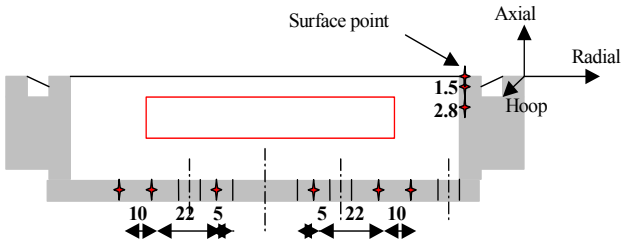

Fig. 2. Geometry of the brake drum - measuring points

Rys. 2. Geometria bębna hamulcowego - punkty obliczeniowe

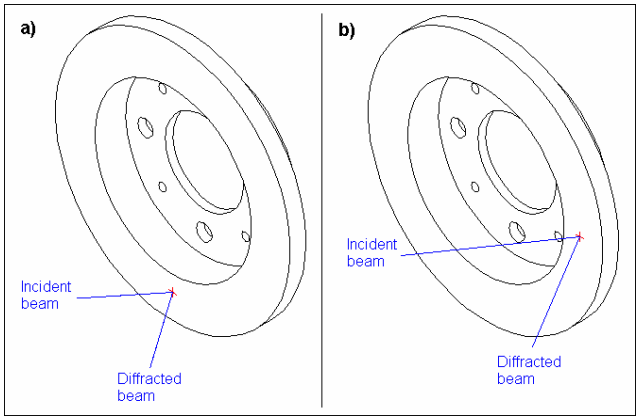

Fig. 3. Lay out of the X-ray diffraction measurement

Rys. 3. Rozkład obliczeń dyfrakcji rentgenowskiej

The results obtained lead to the following conclusions:

1. Large compressive macrostress at the surface of the „wall" exist (–111 MPa in the radial direction). The macrostress decreases just below the surface and become tensile (100 MPa). In the bulk material, for all the other points, the macro stress is tensile and of the order of 100 to 200 MPa. The thermal microstress is larger, especially in the SiC reinforcement were we observe large compressive stresses (–1000 MPa at the top of the wall, –400 MPa in the bottom part).
2. In the wall, the macrostress and the thermal microstress seem to decrease from the surface to the bottom part.

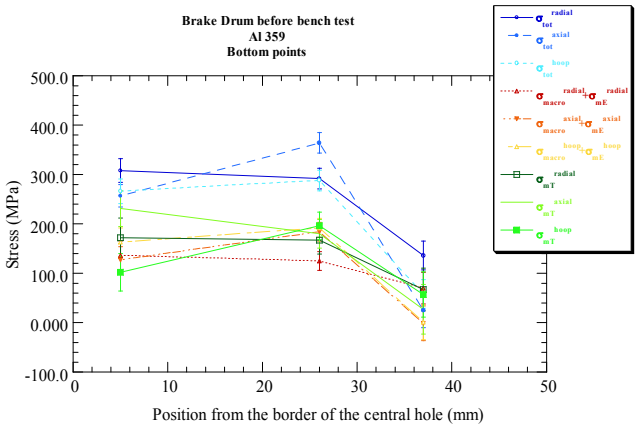

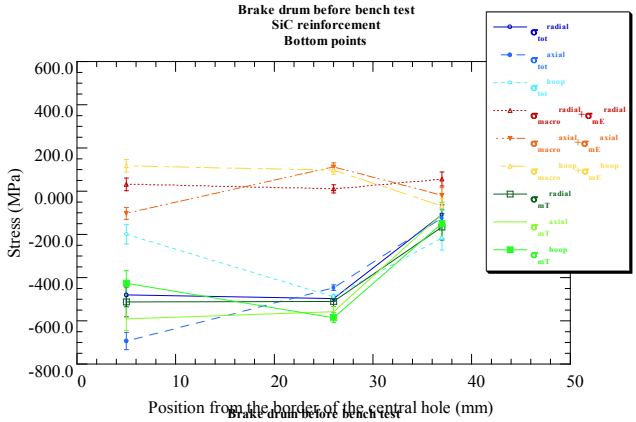

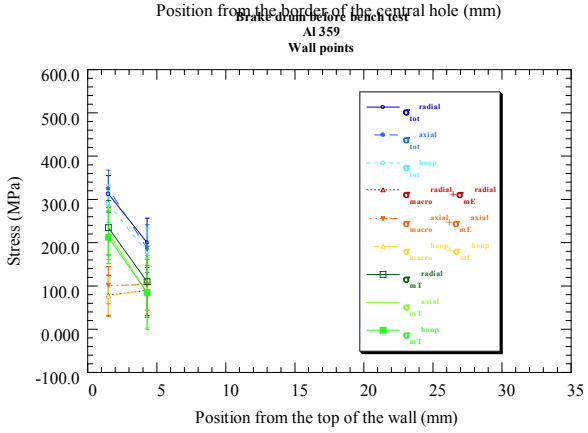

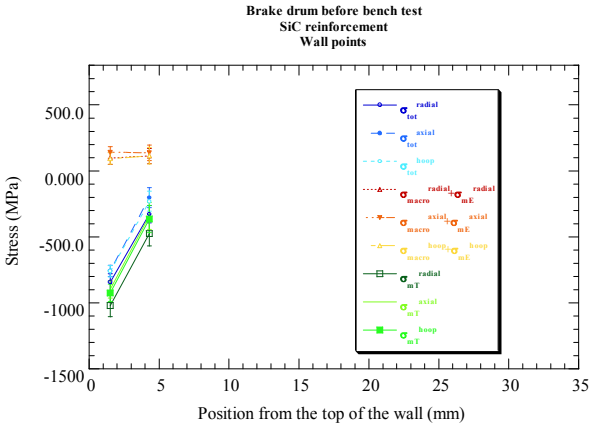

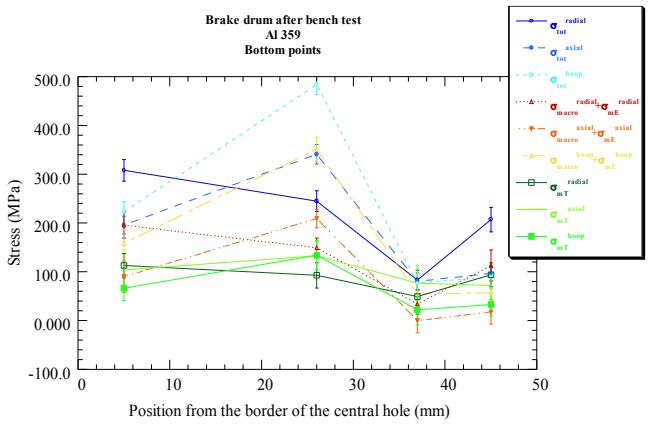
Brake drum after bench test
Al 359
Bottom points
Stress (MPa)
Position from the border of the central hole (mm)

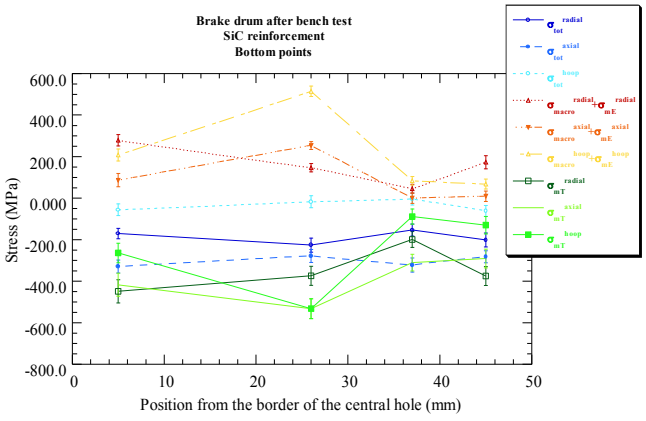
Brake drum after bench test
SiC reinforcement
Bottom points
Stress (MPa)
Position from the border of the central hole (mm)

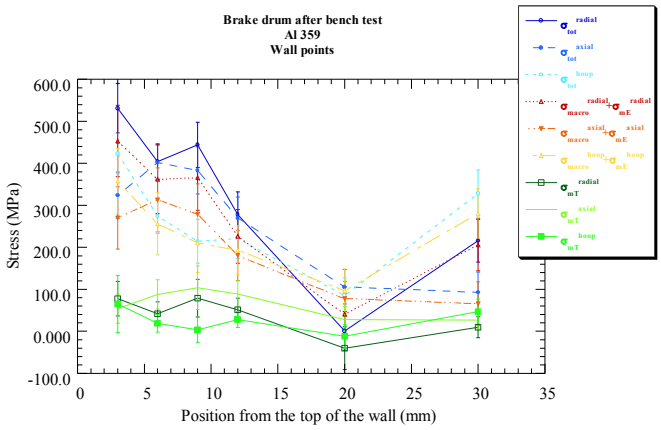
Brake drum after bench test
Al 359
Wall points
Stress (MPa)
Position from the top of the wall (mm)

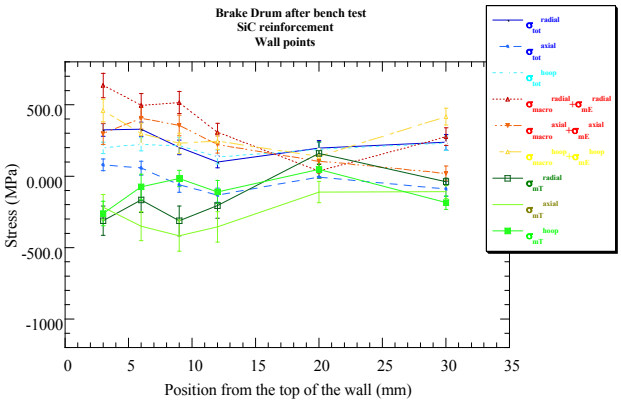
Brake Drum after bench test
SiC reinforcement
Wall points
Stress (MPa)
Position from the top of the wall (mm)

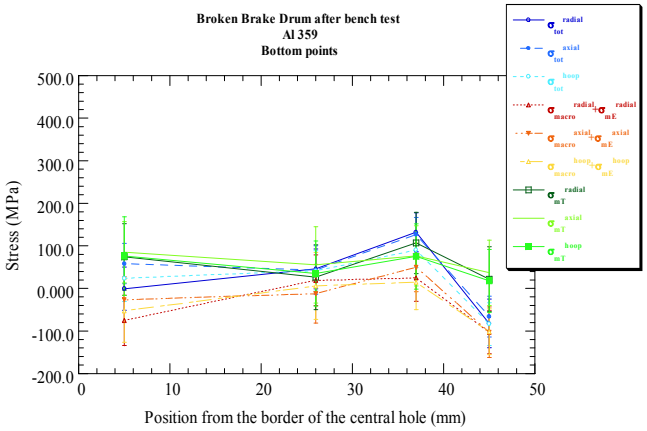
Broken Brake Drum after bench test
Al 359
Bottom points
Stress (MPa)
Position from the border of the central hole (mm)

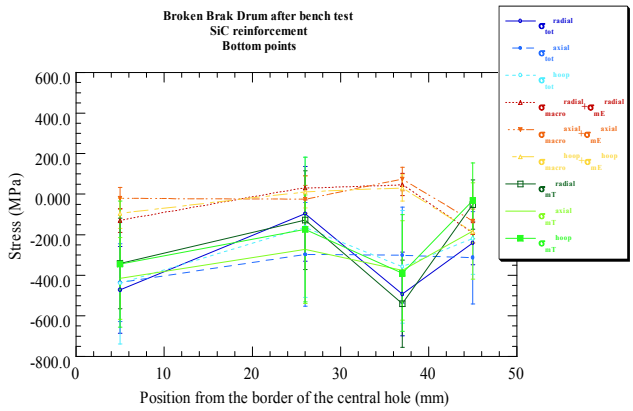
Broken Brak Drum after bench test
SiC reinforcement
Bottom points
Stress (MPa)
Position from the border of the central hole (mm)

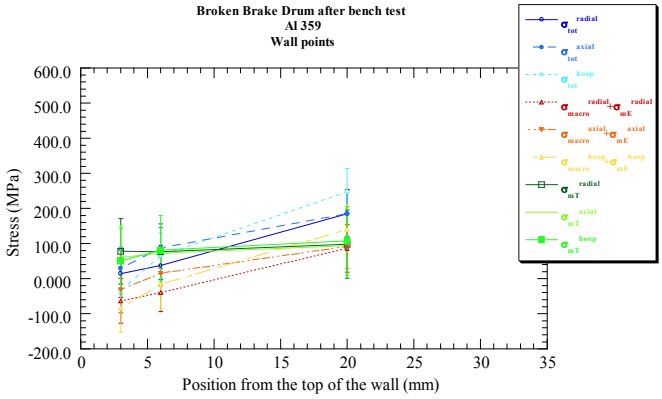
Broken Brake Drum after bench test
Al 359
Wall points
Stress (MPa)
Position from the top of the wall (mm)

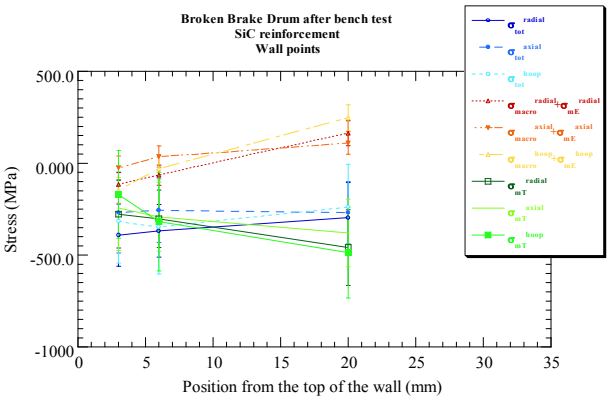
Broken Brake Drum after bench test
SiC reinforcement
Wall points
Stress (MPa)
Position from the top of the wall (mm)

3. The elastic mismatch microstress is negligible.
4. In the bottom part, the macro stress is larger in the centre of the drum (points 6 and 7, > 140 MPa) and decreases going far from the centre (to reach 50 MPa). The thermal microstress has the same behaviour in one side (Al from 194 MPa and SiC from –500 MPa near the central hole to 142 MPa for Al and –400 MPa for SiC near the wall), but not for the symmetric points. In fact, the presence of the small hole (bottom points), near the wall, seems to induce a residual stress at the last point (bottom points, point n°4).

MEASUREMENT AFTER BENCH TEST

We studied the brake drum submitted to the following cycles without breaking:
15,000 N per 2,065,000 cycles
25,000 N per 2,600,000 cycles
30,000 N per 2,500,000 cycles
35,000 N per 2,500,000 cycles

The elastic mismatch micro stresses are of the order of 100 MPa. The main contribution to the total stress is given by the macrostress and the thermal mismatch microstress. The thermal microstresses in the brake drum before bench test are quite the same in the central part of the bottom than in the cast block of A359 + 20% SiC. But in the wall, the stresses are higher. In the brake drum, we observed macrostresses we didn't notice in the cast block.

Residual stress measurements have been carried out also on an other brake drum, broken after 782,000 cycles at 25,000 N. The measuring points are the same as for the non broken brake drum.

In the bottom part, the macrostresses are slightly the same before and after bench test (around 100 MPa). They tends to decrease far from the central hole. They are smaller in the case of the broken brake drum.

The thermal mismatch microstresses, both for aluminium and SiC, are lower after the bench test (around 100 MPa for Al, –400 MPa for SiC). They also decrease far from the central hole (till 94 MPa for Al and –300 MPa for SiC).

In the wall region, the macrostresses are larger after bench test. They are important at the top of the wall (around 400 MPa) and decrease going down along the wall (till 80 MPa). The macrostress increase again at the last point in the radial and hoop direction (to reach 200 and 300 MPa). In the case of the broken brake drum, the macrostresses decreased (–50 MPa at the top of the wall).

The thermal mismatch microstress both for aluminium and SiC is smaller after bench test (70 MPa for Al and –300 MPa for SiC). The thermal mismatch microstress decreases from the top of the wall and going down along the wall (till 20 for Al and –40 MPa for SiC). It increases slightly again for the last point.

The finite element calculation gave results in good agreement with the experience (Fig. 4).

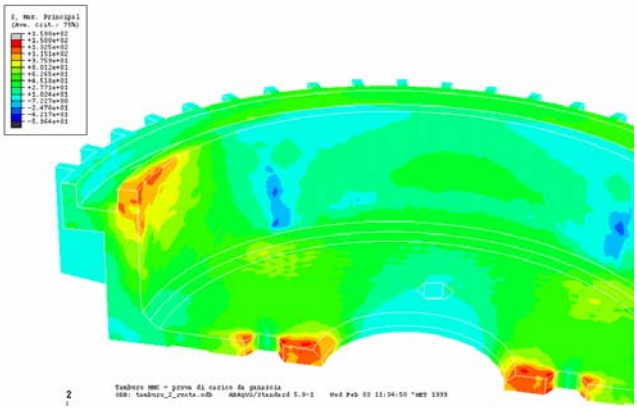

Fig. 4. Finite element calculation: Analysis of the maximum principal stresses

Rys. 4. Obliczenia elementów skończonych - analizy maksimum naprężeń głównych

CONCLUSIONS

As general conclusion, we can assume that after fatigue, the residual stresses in the critical points of the brake drum tends to decrease. We didn't observe any macrostresses in the AA359+20%SiC_p cast sample, however, there are macrostresses in the brake drum, probably due to the fabrication process of the drum. In the bottom part of the drum, the macrostresses are slightly the same before and after bench test; in the wall, they increase after bench test, and decrease in the broken component. The thermal mismatch microstresses in the brake drum are the same as in the cast block.

Recenzent
Krzysztof J. Kurzydłowski